DALTON
FULL PAPER

Mixed cobalt/gold clusters based on octahedral or prismatic Co_6C skeletons

Roser Reina,[a] Olga Riba,[a] Oriol Rossell,[a] Miquel Seco,*[a] Dominique de Montauzon,[c] Maria Angela Pellinghelli,[b] Antonio Tiripicchio,[c] Mercè Font-Bardía[d] and Xavier Solans[d]

[a] *Department de Química Inorgànica, Universitat de Barcelona, Martí i Franquès, 1-11, E-08028 Barcelona, Spain*
[b] *Laboratoire de Chimie de Coordination du CNRS, 205 route de Narbonne, F-31077 Toulouse Cedex, France*
[c] *Dipartimento di Chimica Generale ed Inorganica, Chimica Analitica, Chimica Fisica, Università di Parma, Centro di Studio per la Strutturistica Diffrattometrica del CNR, Parco Area delle Scienze 17A, I-43100 Parma, Italy*
[d] *Department de Cristal·lografia, Mineralogia i Dipòsits Minerals, Universitat de Barcelona, Martí i Franqués s/n, E-08028 Barcelona, Spain*

Received 13th July 2000, Accepted 5th October 2000
First published as an Advance Article on the web 16th November 2000

The reaction of $AuCl(PPh_3)$ in THF with $[Co_6C(CO)_{15}]^{2-}$ **1** afforded $[Co_6C(CO)_{15}\{AuPPh_3\}]^-$ **3**, with a metal skeleton consisting of a Co_6C trigonal prism capped by a $AuPPh_3$ group. **3** incorporated a new $AuPPh_3^+$ fragment giving $[Co_6C(CO)_{13}\{AuPPh_3\}_2]$ **4**. The crystal structure of **4** reveals that the metal skeleton consists of a cobalt octahedron with a face capped by an $Au_2(PPh_3)_2$ unit. The reaction of $AuCl(PPh_3)$ with the anion $[Co_6C(CO)_{13}]^{2-}$, **2** produced the octahedral cluster $[Co_6C(CO)_{13}\{AuPPh_3\}]^-$ in which a face appears to be capped by a $AuPPh_3^+$ group according to the crystal structure determination. This compound reacts with an excess of $AuPPh_3^+$ to give **4**, and produces **3** by reversible reaction with a mild stream of CO. The electrochemical behaviour of these species has been investigated by cyclic voltammetry and coulometry.

Introduction

Numerous studies have examined skeletal rearrangements in transition metal clusters in the belief that they might be related to rearrangements that take place in cluster catalysis. Polyhedral rearrangements are quite varied and a few of them occur spontaneously in solution on the NMR timescale; however, others have to overcome a large energy barrier.[1] This is the case for the interconversion between octahedral and trigonal prismatic cores through a trigonal-twist mechanism that involves the rotation of the two triangles of atoms relative to one another. For example, thermolysis of the trigonal prism $[M_6C(CO)_{15}]^{2-}$ (M = Co or Rh), characterized by a total electron count (TEC) of 90, produces the octahedral 86 electron cluster $[M_6C(CO)_{13}]^{2-}$, which adopts an octahedral geometry.[2–4]

However, the majority of these studies have been carried out on second or third period transition metal clusters. In this paper, therefore, we report the synthesis of a number of mixed gold/cobalt clusters and explore the polyhedral rearrangements that they can undergo as well as the possibility of isolating new skeletal isomers.

Results and discussion

We attempted reactions of the anions $[Co_6C(CO)_{15}]^{2-}$ **1** and $[Co_6C(CO)_{13}]^{2-}$ **2** with the electrophile fragment $AuPPh_3^+$.

(a) Reactions with the trigonal prism $[Co_6C(CO)_{15}]^{2-}$ anion

Although no reports discussing the nucleophilic character of this anion have been published, the ease with which the rhodium congener incorporates metal fragments[5,6] prompted us to treat the cobalt anion with $AuCl(PPh_3)$. The salt $[NEt_4]_2[Co_6C(CO)_{15}]$ was treated with $AuCl(PPh_3)$ in dichloromethane at −12 °C, in the presence of thallium salt as halide abstractor, to form a reddish solution from which crystals of $[NEt_4][Co_6C(CO)_{15}\{AuPPh_3\}]$ **3** were separated in reasonable yields. Compound **3** was characterized by elemental analysis and spectroscopic techniques, but unfortunately we were not able to grow single crystals for a structure determination. The ν(CO) IR bands shifted to higher frequencies (about 20 cm^{-1}) and the ^{31}P NMR spectrum revealed a signal of the phosphine ligand at δ 40, which agrees with the few data that are reported for Co–Au complexes.[7–10] These results suggest that the gold fragment is, in fact, incorporated into the Co_6 metal core. ^1H and ^{13}C NMR spectroscopies showed typical signals for phenyl and CO groups. Unfortunately, we were unable to observe the signal corresponding to the carbido carbon atom. This has previously been the case for other gold clusters synthesized in our laboratory.[11,12] Furthermore, mass spectrometry identified the parent ion peak, suggesting that compound **3** consists of a trigonal-prismatic cobalt core capped on one triangular face by the gold atom. Such a structure in agreement with the expectation that the triangular faces are the most basic sites on the prism surface.[13] and in fact is identical to that reported for the analogous gold/rhodium cluster.[5]

The remaining negative charge on compound **3** might provide the possibility of adding another metal fragment to cap the second triangular face of the trigonal prism skeleton. This reaction has in fact been described elsewhere for the more basic anion $[Rh_6C(CO)_{15}\{AuPPh_3\}]^-$,[5] but it should not be forgotten that a large number of transition metal clusters, particularly iron complexes,[14] are inert to the acceptance of another gold fragment. Thus, when **3** was treated with an excess of $AuCl(PPh_3)$ in CH_2Cl_2 the reaction proceeded cleanly with salt precipitation. Brown crystals of the new

 DOI: 10.1039/b005651k

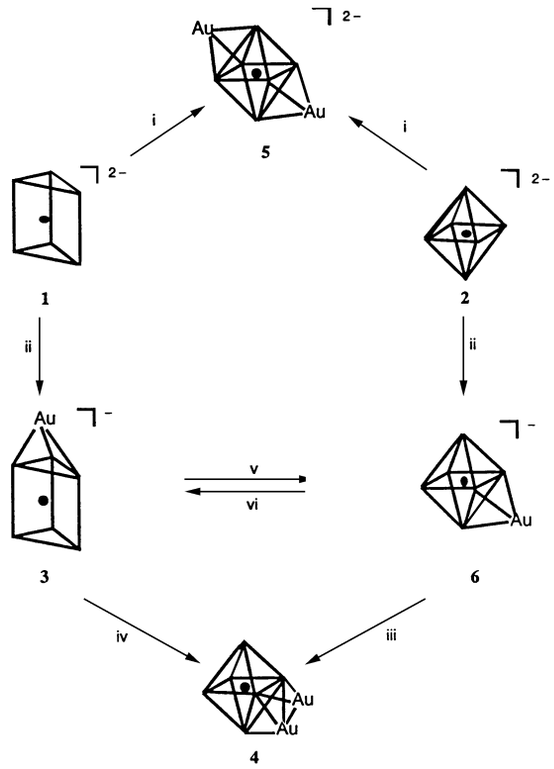

Scheme 1 (i) +2 $AuPPh_3^+$, RT, acetone; (ii) +$AuPPh_3^+$, Tl^+, −12 °C, CH_2Cl_2; (iii) +$AuPPh_3^+$, Tl^+, −12 °C, CH_2Cl_2; (iv) +2 $AuPPh_3^+$, Tl^+, −12 °C, CH_2Cl_2; (v) heat, CH_2Cl_2; (vi) +CO, −12 °C, CH_2Cl_2.

product $[Co_6C(CO)_{13}\{AuPPh_3\}_2]$ **4** were separated (Scheme 1). The highest-wavenumber ν(CO) band of this compound was recorded 15 cm^{-1} higher than that of **3**, indicating a decrease in electron density on the cobalt atoms. On the other hand, the ^{31}P NMR showed a single signal at δ 50.2 with no detectable fluxional variable temperature behaviour. ^1H and ^{13}C NMR spectroscopies revealed typical signals of phenyl and CO ligands and the carbide signal was not observed as mentioned above for complex **3**. FABMS revealed a parent ion peak with only thirteen CO groups. All these data seemed to indicate that a dramatic rearrangement of the original prism geometry had taken place. The determination of the crystal structure of **4** by X-ray methods showed that the metal core can be described as a cobalt octahedron with a face capped by an $Au_2(PPh_3)_2$ system. The octahedral framework accommodates the interstitial C atom. A discussion of bond lengths and angles is not admissible due to the poor quality of the crystals obtained. Nevertheless, the connectivity could be proven. It is remarkable that in this case the trigonal prism/octahedral skeletal rearrangement is induced by insertion of a new gold fragment into **3**, which implies the loss of two carbonyl ligands in order to accomplish the predicted number of electrons by the PSEPT (polyhedral skeletal electron pair theory).[15] The results reported here are even more surprising if we take into account that the trigonal prism $[Rh_6C(CO)_{15}]^{2-}$ reacts with one or two gold units to give the mono- or the di-capped rhodium prism, respectively. This fact can be rationalized if we consider that the ligands on the surface of the smaller Co_6 prism could be much more crowded than on the larger Rh_6 analogue. It seems probable that the driving force behind the skeletal rearrangement reported here is the energy involved in formation of the three new cobalt–cobalt bonds along with the entropic contribution due to the loss of two carbonyl ligands required in the transformation of a trigonal prism into an octahedral core. On the other hand, aureophilicity might, in fact, be responsible for the stabilization of **4**.[16]

In order to detect possible skeletal rearrangements, we treated a dichloromethane solution of compound **4** with a mild stream of CO. It was assumed that the additional four electrons donated by the two CO ligands in the total electron count of the cluster would lead to rearrangement of the octahedral framework into a trigonal prism core. Although IR monitoring in the ν(CO) region revealed shifting of the carbonyl bands to higher frequencies, the resulting product proved to be extremely unstable, rapidly producing $Co_4(CO)_{12}$, the paramagnetic anion $[Co_6C(CO)_{14}]^-$ and other unidentified species, as demonstrated by IR spectroscopy in solution. The presence of $[Co_6C(CO)_{14}]^-$ was corroborated by EPR spectroscopy.[17]

In a last attempt to synthesize the bicapped trigonal prism Au/Co cluster, we decided to carry out the reaction with the same reagents but using acetone instead of dichloromethane. In this new solvent the reaction will only take place at room temperature, according to the IR spectrum, which surprisingly shows a shift of the carbonyl bands at the lowest frequencies (about 40 cm^{-1}). The ν(CO) pattern differed markedly from that shown by the starting anion. The ^{31}P NMR spectrum presented a signal at δ 53, which in this respect is more similar to the behaviour of the octahedral digold compound (δ 50.2) than to the prismatic cluster (δ 40 ppm). ^1H and ^{13}C NMR spectra revealed signals corresponding to phenyls and carbonyl ligands, but again it was not possible to observe the carbide signal. The ESMS spectrum was consistent with the formula $[Co_6C(CO)_{12}\{AuPPh_3\}_2]^{2-}$. For comparison with the structure of the cluster $[Co_6C(CO)_{12}\{HgW(CO)_3Cp\}_2]^{2-}$, which has recently been obtained in our laboratory,[18] we propose a metal framework for $[Co_6C(CO)_{12}\{AuPPh_3\}_2]^{2-}$ **5** consisting of a cobalt octahedron in which two opposite triangular faces are capped by the gold fragment $AuPPh_3$. The formation of **5** from the cobalt anion and $AuPPh_3^+$ leads to the loss of three carbonyl ligands, leaving the resulting product with two negative charges. In fact, **4** and **5** are isoelectronic species. In conclusion, the synthesis of mixed transition metal/cobalt clusters displaying a bicapped trigonal prism geometry was not achieved because of the tendency of the cobalt trigonal prism species to rearrange to the more stable metal octahedral core.

(b) Reactions using the octahedral $[Co_6C(CO)_{13}]^{2-}$ anion

The reaction of $[NEt_4]_2[Co_6C(CO)_{13}]$ **2** with $AuCl(PPh_3)$ in CH_2Cl_2 at −12 °C in the presence of thallium salt gave the cluster $[NEt_4][Co_6C(CO)_{13}\{AuPPh_3\}]$ **6** in good yields, according to spectroscopic data and an X-ray diffraction study (Scheme 1). The ν(CO) bands shifted 25 cm^{-1} higher in comparison with those of **2**. The ^{31}P NMR spectrum showed a signal at δ 54 which agrees with the values found for the other octahedral gold compounds described in this paper. Surprisingly, the typical signals for carbonyl and phenyl groups appear along with the signal corresponding to the carbido carbon atom at δ 467 in the ^{13}C NMR spectrum. This value is consistent with an octahedral geometry while values for prismatic geometries occur around δ 330–360.[13,18] The structure may be regarded as being derived from that of $[Co_6C(CO)_{13}]^{2-}$ following the capping of one triangular face by the $AuPPh_3$ fragment.

Interestingly, compound **6** reacts with a new gold unit to give the octametal cluster **4**, the structure of which has been described above and differs from that of the analogous gold/rhodium cluster.[19] It is remarkable that **4** forms more rapidly *via* **6** than *via* **3**. This can be explained by the fact that the skeletal arrangement required in the second of these processes slows down the reaction.

Given the reasonable stability of species **3** and **6**, it seemed interesting to force skeletal arrangements between both derivatives. Thus, bubbling of carbon monoxide through a dichloromethane solution of **6** leads, in just a few minutes, to a rapid conversion into **3**, according to the IR spectrum in the carbonyl region and the ^{31}P NMR spectrum. On the other hand, warming of **3** leads to release of CO ligands to form **6**. This is the first

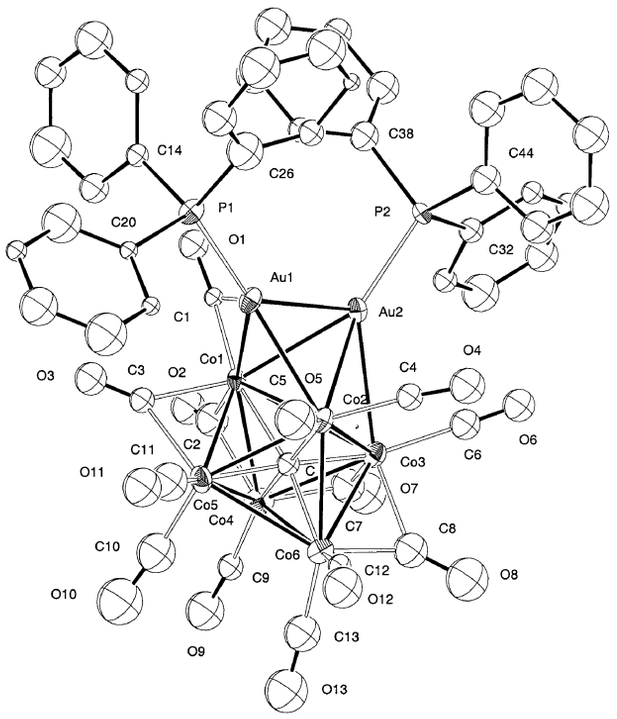

Fig. 1 View of the molecular structure of the cluster $[Co_6C(CO)_{13}\{AuPPh_3\}_2]$ **4** together with the atomic numbering scheme.

reversible skeletal rearrangement reported in the chemistry of octahedral/triangular monocapped metal clusters.

The octahedral anion $[Co_6C(CO)_{13}]^{2-}$ was also treated with an excess of $AuCl(PPh_3)$ in acetone at room temperature in order to examine the influence of the solvent on the course of the reaction. Unexpectedly, after the work up, we were able to isolate crystals of **5** in moderate yields. In this process the incoming $AuPPh_3^+$ groups displace a carbonyl ligand and cap two opposite triangular faces. Evidence of the anionic nature of **5** is provided by its very low solubility in non-polar solvents such as toluene.

In conclusion, while we have shown that although mono- or di-capped octahedral or trigonal prism frameworks can be expected for cobalt clusters, the octahedral structures seem to be more thermodynamically stable than prismatic structures; in fact, we were only able to form a cluster **3** with this latter structure.

Crystal structure of $[Co_6C(CO)_{13}\{AuPPh_3\}_2]$ 4

The molecular structure of compound **4** is shown in Fig. 1 together with the labelling scheme. Significant bond distances and angles are given in Table 1. Even if the structural results are not particularly accurate, given the poor quality and instability of the crystals, they serve our purpose here.

The molecular geometry clearly shows its parentage to the octahedral $[Co_6C(CO)_{13}]^{2-}$ and can be described in terms of the formation of digold derivatives: one, $AuPPh_3$ unit caps a Co_3 face and, a second, a $AuCo_2$ face, so that a Au–Au bond is formed. The strong tendency for Au–Au bond formation causes selectivity in the attachment of the second $AuPPh_3$ unit, which is not added to the cluster on the opposite side of the Co_6 system from that occupied by the first μ_3-$AuPPh_3$ capping fragment. The carbonyl distribution in $[Co_6C(CO)_{13}\{AuPPh_3\}_2]$ is related to that observed in the anion $[Co_6C(CO)_{13}\{AuPPh_3\}]^-$ (see below). The main difference is that the grafting of the second $AuPPh_3$ unit opens one CO bridge ligand. Then, four bridging and nine terminal carbonyl ligands are present. The Co_6 octahedron is highly distorted, and the Co–Co bond lengths fall in the range 2.493(7)–2.992(7) Å. Short bond lengths are associated with the presence of bridging CO ligands, while unbridged distances are longer. This is also observed in the structure of the anion $[Co_6C(CO)_{13}\{AuPPh_3\}]^-$. The Co(1) atom is highly displaced from its ideal octahedral position. It is interesting that it is the sole Co atom bonded to two gold atoms supporting two bridging CO ligands. The Au–Au bond length, 2.842(2) Å, is comparable with values observed in other mixed metal clusters containing this Au–Au system.[11,20]

Table 1 Selected bond lengths (Å) and angles (°) for $[Co_6C(CO)_{13}\{AuPPh_3\}_2]$ **4**

Au(1)–Co(2)	2.641(5)	Co(1)–Co(3)	2.992(7)
Au(1)–Co(1)	2.770(4)	Co(2)–Co(6)	2.627(7)
Au(1)–Au(2)	2.842(2)	Co(2)–Co(3)	2.628(7)
Au(2)–Co(1)	2.666(4)	Co(2)–Co(5)	2.660(6)
Au(2)–Co(3)	2.775(5)	Co(3)–Co(4)	2.493(7)
Au(2)–Co(2)	2.848(5)	Co(3)–Co(6)	2.512(7)
Co(1)–Co(5)	2.496(6)	Co(4)–Co(6)	2.651(7)
Co(1)–Co(4)	2.495(7)	Co(4)–Co(5)	2.712(7)
Co(1)–Co(2)	2.851(6)	Co(5)–Co(6)	2.665(7)
Co(2)–Au(1)–Co(1)	63.56(13)	Au(2)–Co(1)–Co(2)	62.06(13)
Co(1)–Au(1)–Au(2)	56.72(10)	Au(2)–Co(1)–Co(3)	58.39(13)
Co(2)–Au(1)–Au(2)	62.48(11)	Co(3)–Co(2)–Co(1)	66.05(17)
Co(1)–Au(2)–Co(3)	66.70(15)	Au(1)–Co(2)–Au(2)	62.22(11)
Co(1)–Au(2)–Au(1)	60.28(10)	Au(1)–Co(2)–Co(1)	60.43(13)
Co(2)–Au(2)–Au(1)	55.30(10)	Au(2)–Co(2)–Co(1)	55.78(12)
Co(1)–Au(2)–Co(2)	62.17(13)	Au(2)–Co(2)–Co(3)	60.72(15)
Co(2)–Au(2)–Co(3)	55.71(14)	Co(1)–Co(3)–Co(2)	60.56(16)
Co(2)–Co(1)–Co(3)	53.39(15)	Au(2)–Co(3)–Co(2)	63.57(15)
Au(1)–Co(1)–Au(2)	63.00(10)	Au(2)–Co(3)–Co(1)	54.92(13)
Au(1)–Co(1)–Co(2)	56.01(12)		

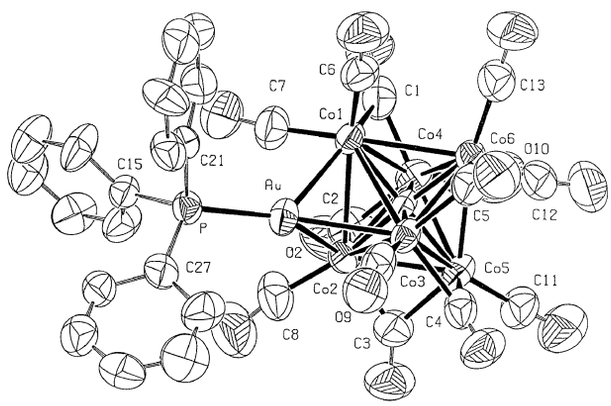

Fig. 2 View of the molecular structure of the cluster anion $[Co_6C(CO)_{13}\{AuPPh_3\}]^-$ **6** together with the atomic numbering scheme.

Crystal structure of $[NEt_4][Co_6C(CO)_{13}\{AuPPh_3\}]$ 6

In the crystals of compound **6**, $[Co_6C(CO)_{13}\{AuPPh_3\}]^-$ anions and NEt_4^+ cations are present. The structure of the anion is shown in Fig. 2 together with the atomic numbering scheme, while the most significant distances and angles are given in Table 2.

The incorporation of the gold fragment does not change the geometry of the initial dianion metal core. In fact, only a greater distortion of the octahedron can be observed. Thus, the structure of compound **6** may be regarded as being derived from that of the dianion $[Co_6C(CO)_{13}]^{2-}$ following capping of a triangular face of the slightly distorted octahedron by the $AuPPh_3$ fragment. The gold fragment interacts through one of the two faces with no Co–Co carbonyl bridged bonds, probably due to steric requirements. The molecular geometry shows that the $AuPPh_3$ ligand adopts an asymmetric μ_3-bonding mode with two short Co–Au distances (mean 2.677(1) Å) and one long (2.850(2) Å). The Co–Au distances are comparable to the average values found in $[FeCo_3(CO)_{12}(\mu_3\text{-}AuPPh_3)]$ (2.714 Å),[21] $[FeCo_3(CO)_{10}(\mu_3\text{-}AuPPh_3)(P(OMe)_3)_2]$ (2.72 Å), $[FeCo_3(CO)_{11}$-

(μ_3-AuPPh$_3$)(PMe$_2$Ph)] (2.71 Å),[22] [RuCo$_3$(CO)$_{12}$(μ_3-AuPPh$_3$)] (2.721 Å),[23] but longer than that in complexes containing two center–two electron Co–Au bonds [Co(CO)$_4${AuPPh$_3$}] (2.50 Å),[24] {[AuCo(CO)$_4$]$_2$(μ-dppfe)} (2.495 Å, dppfe = diphenylphosphinoferrocene),[10] [Co$_2$Au$_2$(CO)$_6$(dppm)$_2$] (2.721 Å).[8] The cobalt atoms Co(1) and Co(3), which are associated with the shorter Co–Au distances, present the longer Co–Co bond length, 2.897(2) Å. As observed in the crystal structure of [Co$_6$C(CO)$_{13}$]$^{2-}$ anion, five carbonyl ligands bridge the metal–metal core edges and the other eight are linearly bonded to the cobalt atoms. The Co–C carbide distances were found to be in the range 1.839(7)–1.903(8) Å, which is higher than that in the [Co$_6$C(CO)$_{13}$]$^{2-}$ anion. Interestingly, a carbide displacement to Co(2) was observed, and to the best of our knowledge, the Co(2)–Au(2) length (2.8499(16) Å) is the longest Co–Au distance reported.

Electrochemical studies

Behaviour of [NEt$_4$][Co$_6$C(CO)$_{15}${AuPPh$_3$}] 3. The Co$_6$-based prismatic complex **3** shows an irreversible reduction and an irreversible oxidation process (see Table 3). When the electrolysis was run at −1.2 V two electrons were exchanged, generating an unstable trianion that decomposed in accordance with reactions (1) and (2). After the coulometry, the resulting anion

$$[Co_6C(CO)_{15}\{AuPPh_3\}]^- + 2e^- \rightleftharpoons [Co_6C(CO)_{15}\{AuPPh_3\}]^{3-} \quad (1)$$

$$[Co_6C(CO)_{15}\{AuPPh_3\}]^{3-} \longrightarrow [Co(CO)_4]^- + [AuPPh_3]^+ + \ldots \quad (2)$$

Table 2 Selected bond lengths (Å) and angles (°) for [NEt$_4$][Co$_6$-C(CO)$_{13}$(AuPPh$_3$)] **6**

Au–P	2.310(2)	Co(3)–Co(5)	2.4920(18)
Au–Co(3)	2.6551(12)	Co(3)–Co(6)	2.5236(19)
Au–Co(1)	2.6997(15)	Co(4)–Co(5)	2.6817(18)
Au–Co(2)	2.8499(16)	Co(4)–Co(6)	2.6636(17)
Co(1)–Co(2)	2.708(2)	Co(5)–Co(6)	2.678(2)
Co(1)–Co(3)	2.8969(17)	Co(1)–C(14)	1.859(7)
Co(1)–Co(4)	2.5039(18)	Co(2)–C(14)	1.839(7)
Co(1)–Co(6)	2.6395(16)	Co(3)–C(14)	1.857(8)
Co(2)–Co(3)	2.8439(16)	Co(4)–C(14)	1.903(8)
Co(2)–Co(5)	2.4999(16)	Co(5)–C(14)	1.876(7)
Co(2)–Co(4)	2.5205(18)	Co(6)–C(14)	1.884(7)
Co(1)–Au–Co(2)	58.35(4)	Au–Co(2)–Co(3)	55.59(3)
Co(1)–Au–Co(3)	65.50(4)	Co(2)–Co(3)–Co(1)	56.29(4)
Co(2)–Au–Co(3)	62.09(4)	Au–Co(3)–Co(1)	57.99(4)
Co(2)–Co(1)–Co(3)	60.86(5)	Au–Co(3)–Co(2)	62.32(4)
Au–Co(1)–Co(3)	56.51(4)	Co(1)–C(14)–Co(5)	173.8(4)
Au–Co(1)–Co(2)	63.60(4)	Co(2)–C(14)–Co(6)	172.5(4)
Co(3)–Co(2)–Co(1)	62.84(4)	Co(3)–C(14)–Co(4)	171.7(4)
Au–Co(2)–Co(1)	58.05(4)		

[Co(CO)$_4$]$^-$ was identified by IR spectroscopy (ν(CO): 1890 cm^{-1}) and by its oxidation peak at 0.20 V.[25] Moreover, cluster **3** also underwent an irreversible oxidation at $E_{p,a}$ = 0.57 V. This is a one-electron process as shown by exhaustive coulometry at controlled potential (0.58 V). The IR spectrum of the resulting solution shows bands corresponding to the paramagnetic anion [Co$_6$C(CO)$_{14}$]$^-$ (ν(CO): 2027vw, 2020vs, 1990sh, 1857m cm^{-1}). This is consistent with the EPR spectrum (g = 2.013).[17] The proposed mechanism is shown in eqns. (3) and (4).

$$[Co_6C(CO)_{15}\{AuPPh_3\}]^- \rightleftharpoons [Co_6C(CO)_{15}\{AuPPh_3\}] + e^- \quad (3)$$

$$[Co_6C(CO)_{15}\{AuPPh_3\}] \longrightarrow [Co_6C(CO)_{14}]^- + [AuPPh_3]^+ + \ldots \quad (4)$$

Behaviour of [NEt$_4$][Co$_6$C(CO)$_{13}${AuPPh$_3$}] 6 and [Co$_6$C-(CO)$_{13}${AuPPh$_3$}$_2$] 4. Both gold octahedral carbide clusters underwent two reversible one-electron reduction steps at a scan rate of 0.1 V s^{-1} (controlled potential coulometries), and presented an irreversible oxidation wave (see Table 3). For the monogold derivative **6** the voltammetry indicates two well defined waves centred at −0.76 and −1.22 V. For each step the diffusion coefficient was near 0.82 × 10^{-6} cm^2 s^{-1}. The electron-transfer rate constants determined by the Nicholson and Shain method[26] for these processes were k° = 10^{-1} and 1.4 × 10^{-1} cm s^{-1}, respectively. All these data point to two reversible processes and the proposed mechanisms are shown in eqns. (5), (6) and (7). When the first reduction was carried out in a cell in the

$$[Co_6C(CO)_{13}\{AuPPh_3\}]^- \underset{-e^-}{\overset{+e^-}{\rightleftharpoons}} [Co_6C(CO)_{13}\{AuPPh_3\}]^{\bullet 2-} \quad (5)$$

$$[Co_6C(CO)_{13}\{AuPPh_3\}]^{\bullet 2-} \underset{-e^-}{\overset{+e^-}{\rightleftharpoons}} [Co_6C(CO)_{13}\{AuPPh_3\}]^{3-} \quad (6)$$

$$[Co_6C(CO)_{13}\{AuPPh_3\}]^{3-} \longrightarrow \text{unidentified products} \quad (7)$$

cavity of the EPR spectrometer at −40 °C it was possible to detect the paramagnetic anion [Co$_6$C(CO)$_{13}${AuPPh$_3$}]$^{\bullet 2-}$, as a wide band centered at 3373 G (g = 2.004). Unfortunately, this species is too unstable to be isolated. When the oxidative electrolysis was carried out at 0.6 V two electrons were exchanged and the only product detected by IR spectroscopy was the neutral cluster [Co$_6$C(CO)$_{13}${μ-AuPPh$_3$}$_2$] **4** (confirmed by CV, see below). The proposed mechanism as in eqns. (8) and (9).

$$[Co_6C(CO)_{13}\{AuPPh_3\}]^- \rightleftharpoons [Co_6C(CO)_{13}\{AuPPh_3\}]^+ + 2e^- \quad (8)$$

Table 3 Cyclic voltammetry data for compounds **3**–**6**[a]

	Reduction				Oxidation			
Compound	$E^{\circ\prime}$/V	ΔE/mV	$i_{p,c}/i_{p,a}$	n	$E^{\circ\prime}$/V	ΔE/mV	$i_{p,a}/i_{p,c}$	n
3	−1.10[b]			2	0.57[c]			1
4	−0.36	72	0.88	1	1.02[c]			1
	−0.92[b]	129	0.70	1				
5	−1.36	80	0.61		0.17	78	0.54	
					0.59	69	0.75	
6	−0.76	71	0.85	1	0.45[c]			2
	−1.22	86	0.75	1				

[a] Scan rate: 0.1 V s^{-1} *vs.* SCE in CH_2Cl_2 or acetone–0.1 M Bu_4NBF_4 at −15 °C. [b] $E_{p,c}$ (irreversible reduction). [c] $E_{p,a}$ (irreversible oxidation). [d] Scan rate: 102 V s^{-1}.

$$[Co_6C(CO)_{13}\{AuPPh_3\}]^+ \longrightarrow [Co_6C(CO)_{13}\{AuPPh_3\}_2] + \ldots \quad (9)$$

For the neutral digold compound **4** the voltammetry of the first reduction showed a well defined wave at −0.36 V with $D = 10^{-5}$ cm^2 s^{-1} and $k^\circ = 2.5 \times 10^{-1}$ cm s^{-1}, indicating a quasi-reversible process. The radical formed $[Co_6C(CO)_{13}\{AuPPh_3\}_2]^{\bullet -}$ was detected by EPR ($g = 2.003$), but this reduced form is not stable and cannot be isolated. The second reduction step is not a pure electrochemical step and at high scan rates (102 V s^{-1}) cyclic voltammetry indicated an ECE (electrochemical step-chemical step-electrochemical step) mechanism. This showed an electrochemical reduction at $E^{\circ\prime} = -0.92$ V and $k^\circ = 1.3 \times 10^{-1}$ cm s^{-1} and an irreversible oxidation at $E_{p,a} = -0.65$ V. The intermediate species formed were not stable and therefore could not be identified. Moreover, the IR spectrum of the reduced solution was inconclusive (ν(CO): 1913vs, 1770m cm^{-1}). Cluster **4** also underwent an irreversible oxidation at 1.02 V. Exhaustive coulometric oxidation at 1.1 V requires one electron per mol of the complex. The IR spectrum of the resultant solution and cyclic voltammetry indicated the formation of $Co_4(CO)_{12}$ (ν(CO): 2063s, 2034vs, 1860m cm^{-1}; $E^{\circ\prime} = -0.36$ V).[27] The proposed mechanism is as in eqns. (10) and (11).

$$[Co_6C(CO)_{13}\{AuPPh_3\}_2] \rightleftharpoons [Co_6C(CO)_{13}\{AuPPh_3\}_2]^{\bullet +} + e^- \quad (10)$$

$$[Co_6C(CO)_{13}\{AuPPh_3\}_2]^{\bullet +} \longrightarrow [Co_4(CO)_{12}] + \ldots \quad (11)$$

Behaviour of $[NEt_4]_2[Co_6C(CO)_{12}\{AuPPh_3\}_2]$ 5. The octahedral dianion **5** exhibited three electrode processes. A quasi-reversible reduction at $E^{\circ\prime} = -1.36$ V and two quasi-reversible oxidation processes at $E^{\circ\prime} = 0.17$ and 0.59 V. However, the great instability of this compound in solution even at −15 °C ruled out an exhaustive electrochemical study.

In summary, we observed interesting differences between the two geometries: the prismatic cluster showed an irreversible reduction while the octahedral species presented reversible reductions. This difference might suggest that prismatic clusters are more unstable than octahedral species. The irreversibility in the reduction was also observed for $[Co_6C(CO)_{15}]^{2-}$ **1**.[28]

Experimental

All manipulations were performed under an atmosphere of prepurified N_2 with standard Schlenk techniques, and all solvents distilled from appropriate drying agents. Infrared spectra were recorded in CH_2Cl_2 or acetone solutions on a FT-IR 520 Nicolet spectrophotometer, ^{1}H, ^{13}C-{^{1}H} and ^{31}P-{^{1}H} NMR spectra on Bruker DRX 250 and Varian XL-500 spectrometers (δ(TMS) 0.0 and δ(85% H_3PO_4) 0.0), FABMS and ESMS spectra on a Fisions VG Quattro spectrometer with CH_2Cl_2 methanol or acetone as solvent, and EPR spectra on a Bruker ESP 300 E spectrometer in X-band mode at 100 K with the standard Bruker VT 1000 cryostat. Compounds $AuCl(PPh_3)$,[29] $[NEt_4]_2[Co_6C(CO)_{15}]$[13] and $[NEt_4]_2[Co_6C(CO)_{13}]$[2] were synthesized as previously described. The synthetic methodology described below corresponds to those reactions that afford the best yields and purest final products. Moreover, all reactions were monitored by IR spectroscopy.

Syntheses

$[NEt_4][Co_6C(CO)_{15}\{AuPPh_3\}]$ 3. Solid $AuCl(PPh_3)$ (0.13 g, 0.28 mmol) and $TlBF_4$ (0.08 g, 0.28 mmol) were added to a solution of $[NEt_4]_2[Co_6C(CO)_{15}]$ **1** (0.30 g, 0.28 mmol) in CH_2Cl_2 (15 mL) at −12 °C. The solution was stirred for 1 hour and the salts filtered off. After the solution was layered with diethyl ether (10 mL) and cooled overnight (−30 °C) red needles of compound **3** were obtained (0.18 g, 46% yield) (Found: C, 36.70; H, 2.60; N, 1.05. $C_{42}H_{35}AuCo_6NO_{15}P$ requires C, 36.68; H, 2.56; N, 1.02%); $\tilde{\nu}_{max}$/cm^{-1} (CO) 2044m, 2004vs and 1850m (CH_2Cl_2); δ_H (295 K, CD_2Cl_2) 7.5–7.1 (m, 15H, $P(C_6H_5)_3$), 3.2 (q, 8H, CH_2) and 1.3 (tt, 12H, CH_3); δ_C (295 K, CD_2Cl_2) 226.7 (m, CO), 222.7 (m, CO), 134.3–129.5 (m, C_6H_5), 53.2 (s, CH_2) and 7.3 (s, CH_3); δ_P (295 K, CD_2Cl_2) 40.0 (s, $P(C_6H_5)_3$); ESMS *m*/*z* (M^-) 1244.

$[NEt_4][Co_6C(CO)_{13}\{AuPPh_3\}]$ 6. Solid $AuCl(PPh_3)$ (0.15 g, 0.30 mmol) and $TlBF_4$ (0.09 g, 0.30 mmol) were added to a solution of $[NEt_4]_2[Co_6C(CO)_{13}]$ **2** (0.30 g, 0.30 mmol) in CH_2Cl_2 (15 mL) at −12 °C. The mixture was stirred for 1 h and addition of 5 mL of diethyl ether caused precipitation of the salts. After filtration the solution was layered with 10 mL of diethyl ether and cooled overnight at −30 °C. Red-brown crystals of compound **6** were obtained (0.18 g, 48% yield) (Found: C, 36.70; H, 2.71; N, 1.09. $C_{40}H_{35}AuCo_6NO_{13}P$ requires C, 36.42; H, 2.67; N, 1.06%); $\tilde{\nu}_{max}$/cm^{-1} (CO) 2041m, 1989vs and 1824m (CH_2Cl_2); δ_H (295 K, CD_2Cl_2) 7.4 (m, 15H, $P(C_6H_5)_3$), 3.1 (q, 8H, CH_2) and 1.2 (tt, 12H, CH_3); δ_C (296 K, CD_2Cl_2) 467.0 (s, C), 226.8 (s, CO), 223.2 (s, CO), 134.3–129.2 (m, C_6H_5), 53.0 (s, CH_2) and 7.6 (s, CH_3); δ_P (295 K, CD_2Cl_2) 54.0 (s, $P(C_6H_5)_3$); ESMS *m*/*z* (M^-) 1189.

$[Co_6C(CO)_{13}\{AuPPh_3\}_2]$ 4. To a solution of $[NEt_4]$-$[Co_6C(CO)_{13}\{\mu\text{-}AuPPh_3\}]$ **6** in CH_2Cl_2 (15 mL) at −12 °C, solid $AuCl(PPh_3)$ (0.15 g, 0.30 mmol) and $TlBF_4$ (0.09 g, 0.30 mmol) were added. After 1 h of stirring, the mixture was filtered and the solvent evaporated to dryness *in vacuo*. The product was extracted with 15 mL of toluene and layered with 10 mL of hexane. When the mixture stood at −30 °C for at least 5 h dark brown crystals were formed (0.15 g, 32% yield) (Found: C, 36.50; H, 1.86; $C_5H_{30}Au_2Co_6O_{13}P_2$ requires C, 36.43; H, 1.83%); $\tilde{\nu}_{max}$/cm^{-1} (CO) 2059m, 2019vs and 1858m (CH_2Cl_2); δ_H (295 K, CD_2Cl_2) 7.6–7.3 (m, 15H, $P(C_6H_5)_3$); δ_C (295 K, CD_2Cl_2) 216.8 (m, CO) and 134.1–129.4 (m, C_6H_5); δ_P (295 K, CD_2Cl_2) 50.2 (s, $P(C_6H_5)_3$); FABMS *m*/*z* (M^-) 1649.

$[NEt_4]_2[Co_6C(CO)_{12}\{AuPPh_3\}_2]$ 5. To a solution of $[NEt_4]_2$-$[Co_6C(CO)_{15}]$ **1** (0.30 g, 0.28 mmol) in acetone (30 mL) at room temperature solid $AuCl(PPh_3)$ (0.13 g, 0.28 mmol) was added. After stirring the mixture for 1 hour an equivalent of $AuCl(PPh_3)$ (0.13 g) was added. The resulting solution was stirred for 8 hours and the salts filtered off. Addition of hexane (4 × 5 mL) gave a red-brown microcrystalline solid of compound **5** (0.10 g, 19% yield) (Found: C, 45.60; H, 3.79; N, 1.53. $C_{65}H_{70}Au_2Co_6N_2O_{12}P_2$ requires C, 45.51; H, 3.75; N, 1.49%); $\tilde{\nu}_{max}$/cm^{-1} (CO) 1983w, 1942vs and 1810m (acetone); δ_H (295 K, CD_2Cl_2) 7.4–7.2 (m, 30H, $P(C_6H_5)_3$), 3.4 (q, 16H, CH_2) and 1.3 (tt, 24H, CH_3); δ_C (295 K, CD_2Cl_2) 134.8–129.2 (m, C_6H_5), 52.8 (s, CH_2) and 7.5 (s, CH_3); δ_P (295 K, CD_2Cl_2) 53.0 (s, $P(C_6H_5)_3$); ESMS *m*/*z* (M/2) 810.

Electrochemical measurements

Electrochemical measurements were carried out with an Electrokemat potentiostat[30] at −15 °C with CH_2Cl_2 as solvent except in the case of compound **5**, in an airtight three-electrode cell connected to a vacuum argon line. The reference electrode consisted of a saturated calomel electrode (SCE) separated from the non-aqueous solutions by a bridge compartment. The counter electrode was a spiral of *ca.* 1 cm^2 apparent surface area, made of a platinum wire 8 cm in length and 0.5 cm in diameter. The working electrode was a gold wire (0.125 mm diameter). For electrolysis a gold wire (1 mm in diameter, 10 cm in length) or a platinum foil was used. $E^{\circ\prime}$ values were determined as the average of the cathodic and anodic peak potentials, *i.e.* $(E_{p,c} + E_{p,a})/2$. The supporting electrolyte (n-Bu_4N)[BF_4] (Fluka, electrochemical grade) was

Table 4 Crystal data and structure refinement for $[Co_6C(CO)_{13}\{AuPPh_3\}_2]$ **4** and $[NEt_4][Co_6C(CO)_{13}\{AuPPh_3\}]$ **6**

	4	**6**
Empirical formula	$C_{50}H_{30}Au_2Co_6O_{13}P_2$	$C_{40}H_{35}AuCo_6NO_{13}P$
Formula weight	1648.19	1319.21
T/K	293(2)	293(2)
Crystal system, space group	Triclinic, $P\bar{1}$	Monoclinic, $P2_1/c$
a/Å	13.837(2)	9.630(6)
b/Å	14.443(6)	22.128(7)
c/Å	16.918(5)	21.598(8)
α/°	80.90(2)	
β/°	81.53(2)	95.44(3)
γ/°	62.38(2)	
V/Å^3	21947.4(16)	4582(4)
Z	2	4
μ/mm^{-1}	6.711	5.404
Reflections collected/ unique	7181/7181	13689/13297 [R(int) = 0.0749]
Final $R1$, $wR2$ [$I > 2\sigma(I)$]	0.1327, 0.3151	0.0492, 0.1030
(all data)	0.2108, 0.3647	0.1933, 0.1400

used as received. Dichloromethane and acetone were freshly distilled prior to use. The solutions used during the electrochemical studies were typically 4×10^{-4} M in the organometallic complex and 0.1 M in (n-Bu_4N)[BF_4]. Under the same conditions, ferrocene was oxidized at $E^{\circ\prime} = 0.42$ V *vs.* SCE and the peak potential separation ΔE was 60 mV. The cyclic voltammetries were run at $v = 0.1$ V s^{-1}.

Crystal structure determinations of $[Co_6C(CO)_{13}\{AuPPh_3\}_2]$ 4 and $[NEt_4][Co_6C(CO)_{13}\{AuPPh_3\}]$ 6

Crystallographic data for both structures are summarized in Table 4. A prismatic crystal of compound **6** was selected and mounted on an Enraf-Nonius CAD4 four-circle diffractometer. Owing to the instability and as a result the very rapid decay of the reflections, several crystals of **4** were mounted on a Philips PW 1100 diffractometer and used for data collection. An empirical correction for absorption was applied to both compounds.[31]

The structures were solved by direct methods, using the SHELXL 97 computer program,[32] and refined by full-matrix least squares against F_o^2. Only the Au, Co and P atoms of compound **4** were refined anisotropically, the remaining atoms being refined isotropically in all stages of refinement, whereas all non-hydrogen atoms of **6** were refined anisotropically. All hydrogen atoms were placed at their geometrically calculated positions and refined with an overall isotropic thermal parameter using a riding model.

CCDC reference number 186/2219.

See http://www.rsc.org/suppdata/dt/b0/b005651k/ for crystallographic files in .cif format.

Acknowledgements

We thank R. Costa for helpful discussions. Financial support for this work was generously given by the DGICYT (Project PB96-0174) and by the CIRIT (Project 1997SGR 00174).

References

1 O. Rossell, M. Seco and G. Segalés, in *Metal Clusters in Chemistry*, eds. P. Braunstein, L. Oro and P. R. Raithby, Wiley-VCH, Weinheim, 1999, vol. 2, pp. 1053–1072.
2 V. G. Albano, D. Braga and S, Martinengo, *J. Chem. Soc.*, *Dalton Trans.*, 1986, 981.
3 V. G. Albano, D. Braga and S. Martinengo, *J. Chem. Soc.*, *Dalton Trans.*, 1981, 717.
4 B. T. Heaton, L. Strona and S. Martinengo, *J. Organomet. Chem.*, 1981, **215**, 415.
5 A. Fumagalli, S. Martinengo, V. G. Albano and D. Braga, *J. Chem. Soc.*, *Dalton Trans.*, 1988, 1237.
6 B. T. Heaton, L. Strona, S. Martinengo, D. Strumolo, V. G. Albano and D. Braga, *J. Chem. Soc.*, *Dalton Trans.*, 1983, 2175.
7 J. W. A. Velden, J. J. Bour, W. P. Bousman and J. H. Noordik, *Inorg. Chem.*, 1983, **22**, 1913; J. Bashkin, C. E. Briant, D. M. P. Mingos and R. W. M. Wardle, *Transition Met. Chem.*, 1985, **10**, 113; Y. Katsukawa, S. Onaka, Y. Yamada and M. Yamashita, *Inorg. Chim. Acta*, 1999, **294**, 255.
8 A. Pons, O. Rossell, M. Seco and A. Perales, *Organometallics*, 1995, **14**, 555.
9 A. Pons, O. Rossell, M. Seco, X. Solans and M. Font-Bardía, *J. Organomet. Chem.*, 1996, **514**, 177.
10 S. Onaka, Y. Katsukawa and M. Yamashita, *J. Organomet. Chem.*, 1998, **564**, 249.
11 O. Rossell, M. Seco, G. Segalés, M. A. Pellinghelli and A. Tiripicchio, *J. Organomet. Chem.*, 1998, **571**, 123.
12 R. Reina, O. Riba, O. Rossell, M. Seco, P. Gómez-Sal, A. Martín, D. de Montauzon and A. Mari, *Organometallics*, 1998, **17**, 4127.
13 S. Martinengo, D. Strumolo, P. Chini, V. G. Albano and D. Braga, *J. Chem. Soc.*, *Dalton Trans.*, 1985, 35.
14 O. Rossell, M. Seco and P. G. Jones, *Inorg. Chem.*, 1990, **29**, 348; O. Rossell, M. Seco, R. Reina, M. Font-Bardía and X. Solans, *Organometallics*, 1994, **13**, 2127; O. Rossell, M. Seco, G. Segalés, S. Alvarez, M. A. Pellinghelli, A. Tiripicchio and D. de Montauzon, *Organometallics*, 1997, **16**, 236.
15 D. M. P. Mingos and D. J. Wales, *Introduction to Cluster Chemistry*, Prentice Hall International, London, 1990.
16 H. Schmidbauer, *Chem. Soc. Rev.*, 1995, **24**, 391.
17 V. G. Albano, P. Chini, G. Ciani, M. Sansoni, D. Strumolo, B. T. Heaton and S. Martinengo, *J. Am. Chem. Soc.*, 1976, **98**, 5027.
18 R. Reina, O. Riba, O. Rossell and M. Seco, unpublished work.
19 A. Fumagalli, S. Martinengo, V. G. Albano, D. Braga and F. Grepioni, *J. Chem. Soc.*, *Dalton Trans.*, 1989, 2343.
20 I. D. Salter, in *Comprehensive Organometallic Chemistry*, eds. E. W. Abel, F. G. A. Stone and G. Wilkinson, Pergamon Press, Elmsford, NY, 1995, vol. 10, ch. 5.
21 J. W. Lauher and K. Wald, *J. Am. Chem. Soc.*, 1981, **103**, 7648.
22 A. A. Low and J. W. Lauher, *Inorg. Chem.*, 1987, **26**, 3863.
23 P. Braunstein, J. Rosé, A. Dedieu, Y. Dusausoy, J. P. Mangeot, A. Tiripicchio and M. Tiripicchio Camellini, *J. Chem. Soc.*, *Dalton Trans.*, 1986, 225.
24 T. L. Blundell and H. M. Powell, *J. Chem. Soc. A*, 1971, 1685.
25 P. Lemoine, A. Giraudeau, M. Gross, R. Bender and P. Braunstein, *J. Chem. Soc.*, *Dalton Trans.*, 1981, 2059.
26 R. S. Nicholson, *Anal. Chem.*, 1965, **36**, 1351; R. S. Nicholson and I. Shain, *Anal. Chem.*, 1966, **37**, 706.
27 J. Rimmelin, P. Lemoine, M. Gross and D. de Montauzon, *Nouv. J. Chem.*, 1983, **7**, 453; J. Rimmelin, P. Lemoine, M. Gross, A. Bahsoun and J. A. Osborn, *Nouv. J. Chem.*, 1985, **9**, 181.
28 J. Rimmelin, P. Lemoine, M. Gross, R. Mathieu and D. de Montauzon, *J. Organomet. Chem.*, 1986, **309**, 355.
29 C. Kowala and J. M. Swan, *Aust. J. Chem.*, 1966, **19**, 547.
30 P. Cassoux, R. Dartiguepeyron, D. de Montauzon, J. B. Tommasino and P. L. Fabre, *Actual Chim.*, 1994, **1**, 49.
31 N. Walker and D. Stuart, *Acta Crystallogr.*, *Sect. A*, 1983, **39**, 158.
32 G. M. Sheldrick, SHELXL 97, A computer program for determination of crystal structure, University of Göttingen, 1997.